Available online at www.sciencedirect.com

SCIENCE DIRECT®

Nuclear Medicine and Biology 32 (2005) 719–725

NUCLEAR MEDICINE — AND — BIOLOGY

www.elsevier.com/locate/nucmedbio

Resolution, sensitivity and precision with autoradiography and small animal positron emission tomography: implications for functional brain imaging in animal research

Kathleen C. Schmidt*, Carolyn Beebe Smith

Unit on Neuroadaptation and Protein Metabolism, Laboratory of Cerebral Metabolism, National Institute of Mental Health, Bethesda, MD 20892-4030, USA

Received 22 March 2005; received in revised form 22 April 2005; accepted 23 April 2005

Abstract

Quantitative autoradiographic methods for *in vivo* measurement of regional rates of cerebral blood flow, glucose metabolism, and protein synthesis contribute significantly to our understanding of phsysiological and biochemical responses of the brain to changes in the environment. A disadvantage of these autoradiographic methods is that experimental animals can be studied only once. With the advent of small animal positron emission tomography (PET) and with increases in the sensitivity and spatial resolution of scanners it is now possible to use adaptations of these methods in experimental animals with PET. These developments allow repeated studies of the same animal, including studies of the same animal under different conditions, and longitudinal studies. In this review we summarize the tradeoffs between the use of autoradiography and small animal PET for functional brain imaging studies in animal research.
© 2005 Elsevier Inc. All rights reserved.

Keywords: Positron emission tomography; Cerebral blood flow; Cerebral glucose utilization; Cerebral protein synthesis

1. Introduction

Since the earliest positron emission tomography (PET) scanners made their debut in the 1960s, there have been numerous technological improvements that allow brain imaging with increasing spatial resolution. PET scanners optimized specifically for use with small animals have been designed and reconstruction algorithms advanced such that we can now expect to examine tissues with a spatial resolution less than 2 mm full-width at half maximum (FWHM). Newer detector materials and design configurations are providing increasing sensitivity. Much of the focus to date has been on the development of new tracers and improvements in instrumentation; indeed, current small animal PET imaging technologies have opened up a number of new investigative possibilities. Small animal PET is however, not suitable for all functional brain imaging studies. In the present discussion, we contrast the strengths and intrinsic limitations of PET with those of autoradiographic techniques in order to try to identify applications better suited to each method.

2. Measuring the rate of a biologic process

It is important to emphasize that the goal of functional brain imaging is not the generation of images per se, but rather to gain greater understanding of the physiology and biochemistry of the brain. Methods are well established for the measurement of regional cerebral blood flow (rCBF) [1], regional cerebral glucose metabolism ($rCMR_{glc}$) [2] and regional rates of cerebral protein synthesis (rCPS) [3] with radiolabeled tracers and quantitative autoradiography. Measurement of rCBF [4] and $rCMR_{glc}$ [5] with PET has also been possible for more than two decades, and a recently quantitative method for measurement of rCPS with PET has been proposed [6] and validated [7]. The methods share the common requirement that tracer activity in the blood and the brain be measured following introduction of the radiotracer into the blood. A mathematical relationship between the measured blood and brain activities is used to determine the absolute rate of the underlying biologic process of interest.

The ability to measure absolute rates of a well-defined biologic process is essential when different individuals or groups are to be compared. In this respect, quantitative autoradiography and PET functional imaging methods contrast with other methods in which only relative rates

* Corresponding author. Tel.: +1 301 402 3119; fax: +1 301 480 1668.
E-mail address: schmidtk@intra.nimh.nih.gov (K.C. Schmidt).

0969-8051/$ – see front matter © 2005 Elsevier Inc. All rights reserved.
doi:10.1016/j.nucmedbio.2005.04.020

of various processes can be determined. For example, functional MRI based on the blood oxygenation level-dependent effect, i.e., the BOLD effects, is used to quantify signals related to cerebral hemodynamics, but the signals are influenced by a number of biologic processes that determine the amount of deoxygenated hemoglobin in the image voxel (e.g., blood flow, cerebral metabolic rate of oxygen, blood volume, relative amount of arterial and venous blood in the voxel) [8] and quantification is restricted to measuring differences in signal strength under differing conditions in a single individual. Laser Doppler flowmetry can be used to measure changes in blood velocity from baseline values but lacks the possibility for calibration to absolute levels of CBF [9].

A look at the success of one of the earliest PET methods, the [^{18}F]fluorodeoxyglucose ([^{18}F]FDG) method [5], is illustrative of the potentials of functional brain imaging with PET. The method was developed with the expectation that a protocol to detect alterations in local cerebral energy metabolism would enable the identification of regions in the brain involved in normal functions and those affected in neurological and mental disorders. Because of the close relationship between local functional activity and energy metabolism [10], evoked metabolic responses promised to be a potent tool to localize the sites of specific functions within the brain. The method does, to a considerable extent, achieve these goals due to two of its key properties: the ability to localize metabolic changes and the ability to fully quantify functional activity in different individuals or groups. It is with respect to these features, localization and quantification of function, that the current PET technologies must be evaluated for use in brain functional imaging.

3. Functional brain imaging with quantitative autoradiography

Autoradiography allows measurement of tissue activity with a spatial resolution that is approximately an order of magnitude higher than is possible with PET, on the order of less than a few hundred microns versus a few millimeters with PET. It is also possible to conduct the studies in freely moving, conscious, behaving animals. The major disadvantage is that an animal can only be studied once. Longitudinal studies and kinetic studies require the use of multiple animals, adding interanimal variability to other sources of variability. When animals are very costly or difficult to produce, availability and expense of animals may become limiting. Another potential disadvantage is that autoradiography is inherently a two-dimensional sampling method, with the plane of view established at the time of tissue sectioning. Brain structures cannot be viewed in different projections without first constructing a three-dimensional volume of the data. Various automated programs have been proposed to align autoradiographic images into a three-dimensional volume (e.g., Ref. [11]), but results are not always entirely satisfactory. Manual alignments are pains-taking and time consuming. Additionally, there may be artifacts in tissue sectioning and, frequently, only a sample of the whole brain is acquired.

3.1. Factors that affect resolution with carbon-14 film autoradiography

The geometrical relationship of the radioactive source and the emulsion, the energy and intensity of the radiation and the characteristics of the photographic emulsion all affect spatial resolution in autoradiography [12]. Autoradiographic resolution is inversely related to the energy of the source β-emissions (i.e., higher energy particles will have a greater range in the photographic emulsion). Carbon-14 (^{14}C) has a low energy β-emission (155 KeV maximum) that gives rise to tracks up to 40 μm from the source, most of them lying within 10 μm [12]. Autoradiographic resolution, $d_{½}$, is defined as the distance from the radioactive source at which film density is half its maximum value. The FWHM therefore is $2d_{½}$, and for intersource activity between two equal point sources to fall to 50% of peak, the sources must be separated by $4d_{½}$. On X-ray film, ^{14}C autoradiographic resolution is approximately 25 μm FWHM. In tissue preparations, diffusion of the tracer can lower the effective spatial resolution below the limit imposed by the energy of ^{14}C and the properties of the X-ray film itself.

The first quantitative autoradiographic functional brain imaging study was the measurement of local CBF in cats [13]. The method was based on the principles of inert gas exchange [14] and used the freely diffusible tracer [^{131}I]trifluoroiodomethane (CF_3I^{131}). CF_3I^{131} had several drawbacks, among them the relatively high energies of the β-emission of the ^{131}I label (608 KeV maximum), the short half life of ^{131}I (~8 days) and the volatility of the tracer that necessitated exposing autoradiographic films at low temperatures. Use of [^{14}C]antipyrine [15] and, subsequently, iodo-[^{14}C]antipyrine [1] resolved these problems, and the low energy β-emission of ^{14}C improved the resolution of the autoradiography. In these experiments, the tracer is distributed according to local CBF, and after 1 min of tracer circulation, the animal is decapitated and the brain is rapidly dissected out and frozen. During the removal of the brain from the cranium, however, diffusion begins to alter the tracer's pattern of distribution. The longer it takes to remove and freeze the brain, the lower the effective resolution of the resulting autoradiograms for localizing rCBF [16].

The original procedure for preparing tissue sections in the quantitative autoradiographic [^{14}C]deoxyglucose ([^{14}C]DG) method for measurement of local cerebral glucose utilization [2] called for dissecting the brain out as rapidly as possible after decapitation of the animal. The brain was frozen and stored at −70°C until sectioned. Brain sections were prepared in a cryostat maintained at −21°C to −22°C, picked up on glass cover slips and dried on a hot plate before being exposed to X-ray film. Diffusion of the water-soluble [^{14}C]DG and its principal metabolic product [^{14}C]DG-6-phosphate can occur during freezing and thaw mounting. The limitation on spatial

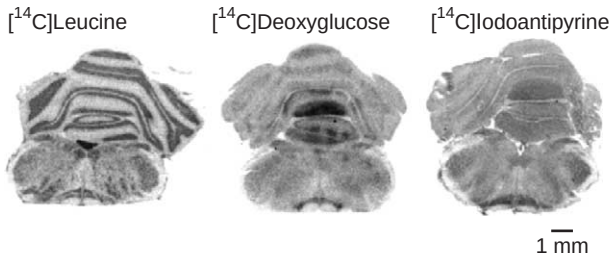

Fig. 1. Film autoradiograms of rat brains labeled with three different ^{14}C tracers. Sections are at the level of the brain stem and cerebellum. Effective spatial resolution depends not only on the isotope but also on the tracer and the method used for tissue preparation. Resolution of [^{14}C]leucine autoradiograms used in the measurement of rCPS is ~25 μm FWHM. Diffusion of label during thaw mounting of tissue sections reduces resolution of [^{14}C]DG autoradiograms (used in measurement of $rCMR_{glc}$) to ~100 μm FWHM. Effective resolution of [^{14}C]iodoantipyrine autoradiograms used in the measurement of rCBF depends on the amount of diffusion that occurs during brain removal before freezing. [^{14}C]Leucine autoradiograms utilized mammography film; X-ray films were used for [^{14}C]DG and [^{14}C]IAP autoradiography.

resolution imposed by diffusion of the label was determined by the following experiment [12]. A plug of uniformly distributed [^{14}C]DG-labeled brain tissue was inserted into a hole drilled in a frozen unlabeled rat brain. Sections were prepared as in a conventional [^{14}C]DG experiment and optical densities in the autoradiogram at various distances from the plug were determined. From the falloff in optical density at increasing distances from the edge of the plug, resolution was determined to be ~100 μm FWHM. Subsequent experience showed that limiting the amount of time the brain remained in the cryostat at −21°C to −22°C was more critical for maintaining spatial resolution than the length of time required for dissection of the brain.

In the quantitative autoradiographic L-[1-^{14}C]leucine method for measuring rCPS, tissue sections are fixed and washed in formalin before autoradiography [3]. This washes out residual free [^{14}C]leucine and fixes the ^{14}C-labeled proteins. As a consequence, spatial resolution is limited only by the geometry and the energy of ^{14}C β-emissions (i.e., approximately 25 μm FWHM) [12].

Film autoradiograms of rat brains labeled with [^{14}C]leucine, [^{14}C]DG and [^{14}C]iodoantipyrine are shown in Fig. 1.

4. Functional brain imaging with small animal PET

The primary advantage of PET studies lies in the ability to perform repeat studies in the same animal. Thus, studies can be designed to use an animal as its own control, reducing both the total number of animals required and the effects of interanimal variability. Longitudinal studies are possible. Additionally, with sufficiently sensitive PET scanners, rapid dynamic scanning is feasible and tracer kinetic modeling can be carried out with data from a single animal. The most obvious disadvantage of PET is its reduced spatial resolution compared with autoradiographic studies. If sensitivity is not sufficient to provide tissue activity measurements with low-enough noise, further reduction in spatial or temporal resolution may prove necessary. A perhaps less obvious disadvantage is the requirement that an animal's head be completely immobilized during PET scanning, often with anesthetic agents that themselves may alter the function that one is trying to measure. Effects of anesthesia and alternative immobilization strategies are discussed in Section 5.

4.1. Factors that affect resolution with small animal PET

The physical limits of spatial resolution in PET due to detector size, photon noncollinearity and positron range (i.e., the distance between the positron emission and the point of annihilation) have been studied for the most commonly used PET isotopes — ^{18}F, ^{13}N, ^{11}C and ^{15}O in water [17]. The fundamental spatial resolution for animal imaging systems (≤20 cm diameter) ranges from ~0.6 mm FWHM for ^{18}F to ~1.6 mm FWHM for ^{15}O [17]. Maximal spatial resolution (i.e., that at the center of the field of view) and sensitivity measured in several commercially available small animal PET scanners [18,19] as well as the Advanced Technology Laboratory Animal Scanner (ATLAS) developed at the National Institutes of Health [20] are shown in Table 1.

We have performed a number of imaging studies with the ATLAS small animal PET, a high-resolution, high-sensitivity scanner [20]. [^{18}F]FDG was used initially in order to explore the feasibility of conducting fully quantitative functional brain imaging studies. The time course of plasma [^{18}F]FDG concentrations was measured from arterial

Table 1
System characteristics of selected small animal PET scanners[a]

Scanner	Field of view		Spatial resolution (FWHM)		Sensitivity (% efficiency)
	Transaxial (cm)	Axial (cm)	Transaxial (mm)	Axial (mm)	
microPET P4 (Concorde Microsystems)	19	7.8	1.8	1.8	1.2 (410–613 keV) 1.4 (350–650 keV) 2.3 (250–750 keV)
Quad HIDAC (Oxford Positron Systems)	17	28	1.0	1.0	1.2–1.6
SHR-7700 (Hammamatsu Photonics)	33	11.4	2.6	3.2	2.3 (two-dimensional) 22.8 (three-dimensional)
ATLAS small animal PET (NIH)	6.8	2	1.5	1.5	1.8 (250–700 keV) 2.7 (100–700 keV)

[a] From Refs. [18–20].

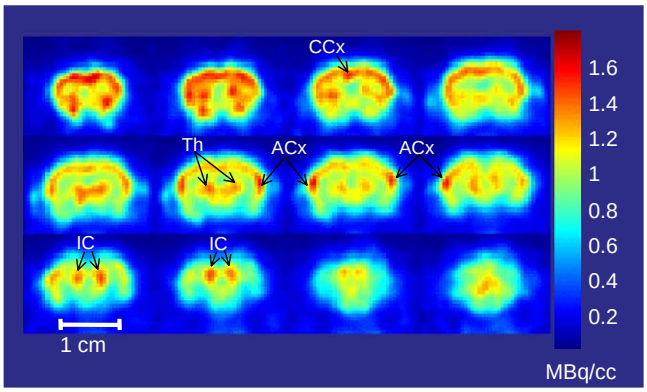

Fig. 2. [^{18}F]FDG PET image of a rat brain acquired with the NIH ATLAS small animal PET scanner. The animal was awake during the 45-min period of tracer uptake prior to scanning. After tracer uptake, the animal was killed and placed on the scanner bed and its head was scanned for a 60-min interval. Note the high cortical uptake of [^{18}F]FDG. The cingulate cortex (CCx), auditory cortex (ACx), thalamus (Th) and inferior colliculus (IC) are clearly visible. Slice thickness is 1.125 mm. Injected dose was 63.9 MBq (1.73 mCi).

blood samples; quantification of $rCMR_{glc}$ then only required localized quantification of ^{18}F brain activities with the ATLAS scanner [21]. An [^{18}F]FDG PET image of rat brain is shown in Fig. 2. The animal was awake during the period of tracer uptake prior to scanning. Note the high cortical uptake of [^{18}F]FDG, in the auditory cortex in particular. The thalamus can be clearly identified, as can the inferior colliculus, a structure that has the highest rate of glucose utilization in conscious rats. Although activity can be localized in a number of structures, the measured activity in gray matter structures is quantitatively lower than the true activity due to the partial volume effects of the PET scanner. In a study of the effects of stroking facial whiskers in adult rats, stimulation-induced increases in tracer uptake determined with [^{18}F]FDG PET in the somatosensory cortex were only ~25–40% of those determined with [^{14}C]DG autoradiography [22].

The sensitivity of the ATLAS scanner is sufficiently high that we were able to conduct kinetic studies in isoflurane-anesthetized rats with [^{18}F]FDG (Table 2; [23]). Kinetic modeling of PET data faces challenges different than those encountered with quantitative autoradiography. Like most tracer kinetic models used with PET, the kinetic model used for the measurement of $rCMR_{glc}$ is based on the assumption that tissue regions are homogeneous, in this case with respect to blood flow, transport of hexoses across the blood–brain barrier, glucose metabolism, FDG phosphorylation and concentrations of FDG, glucose, FDG-6-phosphate and glucose-6-phosphate [2]. Autoradiography provides the means not only for localization but also for visualization and selection for measurement those areas that are relatively homogeneous. The biggest challenge in kinetic modeling with autoradiography is that, in order to obtain the time courses of tissue activity, measurements must be made in a separate group of animals at each time point sampled; interanimal variability may become limiting. With PET, it is possible to follow the time course of activity in a single animal, but the resolution of PET scanning relative to the size of rodent brain structures is not sufficient to avoid including tissues with different rates of blood flow and metabolism within a single voxel or region of interest. Failure to take the kinetic heterogeneity into account leads to errors in the estimates of the kinetic rate constants and estimates of $rCMR_{glc}$ that rely on a kinetic model [24,25]. Strategies to minimize the impact of tissue heterogeneity are required with PET [25–27].

5. Animal head immobilization

In vivo brain imaging with PET requires that an animal's head be immobilized during scanning. Until recently, the method of choice has been the use of anesthetic agents. In rats, most general anesthetics have been shown to produce widespread decreases in local cerebral glucose utilization [28]. rCBF either increases or is unchanged under isoflurane anesthesia [29], is slightly reduced under nitrous oxide anesthesia [30] and is substantially reduced under pentobarbital and chloralose anesthesia [30]. Rates of rCPS show generalized but small decreases under thiopental anesthesia [31]. Use of anesthetic agents in small animal imaging therefore will likely alter the brain function that one is trying to measure. Additionally, anesthesia may affect stimulation-induced changes in brain function. For example, in an autoradiographic study of the effect of alpha-chloralose anesthesia on increases in rCBF and $rCMR_{glc}$ due to whisker stroking in adult rats, Nakao et al. [32] reported stimulation-induced increases of rCBF and

Table 2
Rate constants and regional cerebral glucose metabolism determined with [^{18}F]FDG in isoflurane-anesthetized rats[a]

	K_1* (ml/g/min)	k_2* (min^{-1})	k_3* (min^{-1})	$rCMR_{glc}$ (μmol/100 g/min)
Whole brain	0.184±0.026	0.328±0.033	0.046±0.007	33.1±3.1
Thalamus	0.194±0.034	0.301±0.043	0.045±0.007	37.8±3.8
Cortex	0.238±0.035	0.404±0.040	0.035±0.009	28.9±4.7
Cerebellum	0.205±0.041	0.351±0.056	0.050±0.011	46.5±3.0
Brain stem	0.164±0.032	0.258±0.043	0.064±0.008	36.3±2.8

Rate constants were estimated over a 0- to 60-min interval. K_1* and k_2* are the rate constants for carrier-mediated transport of [^{18}F]FDG from the plasma to the brain and from the brain to the plasma, respectively. k_3* is the rate constant for phosphorylation of [^{18}F]FDG by hexokinase. Values are expressed as mean±S.D., $n=9$.

[a] From Ref. [23].

$rCMR_{glc}$ in the somatosensory cortex that were greatly reduced under anesthesia compared with increases found in conscious animals.

With tracers that are effectively trapped, it may be possible to allow tracer uptake in awake animals before administration of anesthesia and PET scanning. Matsumura et al. [33] reported that [^{18}F]FDG uptake in the whole brain of rats was not significantly affected by administration of anesthesia (ketamine+xylazine or propofol) after 40 min of circulation of the tracer in the awake animals, nor was the pattern of tracer distribution in the brain significantly affected. In this study, however, no arterial blood sampling was performed; hence the effect of the delayed administration of anesthesia on $rCMR_{glc}$ is yet to be fully quantified. Although this approach does not allow kinetic studies, it maintains the possibility of performing longitudinal studies.

PET studies have been carried out in conscious monkeys (e.g., Refs. [34,35]) and cats [36,37] trained to accept head fixation. Recently, a PET study in rats without anesthesia has also been reported [38]. The rats had two plastic tubes affixed to their head by dental cement, and the rat heads were fixed to a wood box using the plastic tubes. The animals underwent 2 weeks of daily training to become acclimated to the apparatus; after training, it was possible to conduct dynamic PET studies for more than 60 min.

An alternative to animal immobilization is designing PET systems that move with the animals. Researchers at Brookhaven National Labs have designed a miniaturized head-mounted PET for conscious rodent brain imaging, although only test images have been published to date [39,40].

6. Studies suitable for small animal PET

The above considerations suggest that functional brain imaging studies suitable for small animal PET are those in which the animals can be trained to accept head fixation, those in which the process studied is relatively unaffected by anesthesia or those studies with tracers that are effectively trapped, such as [^{18}F]FDG. The latter case may allow an awake uptake followed by scanning under anesthesia but precludes kinetic studies. Additionally, in order to examine changes in a functional process due to changes in experimental condition, the magnitude and/or extent of the change must be sufficient to detect with the PET scanner to be used.

7. Use of autoradiographic data in designing small animal PET studies

The effect of object size on quantification with PET has been extensively studied. Various test objects filled with a positron-emitting compound are placed in the scanner and percent recovery of the known activity is measured. For a hot cylinder in a cold background, for example, obtaining a recovery coefficient greater than 80% requires a cylinder greater than 1.5 FWHM in diameter [41]. From these measurements, activity "spilled out" to the surrounding areas can be determined. Since there is no activity present in the surrounding areas during the test, however, it cannot be used for determining activity that will be "spilled in" from surrounding areas in an actual brain imaging study. Use of phantoms with different spaces filled with different activities represents a refinement to the test approach, but phantoms are, of necessity, a simplification of the distribution of activity in the living brain. Detailed distributional data from autoradiographic studies with the ^{14}C-labeled counterpart of the PET tracer have been used to estimate the precision of PET measurements by computationally matching the resolution of the autoradiographic images to that of

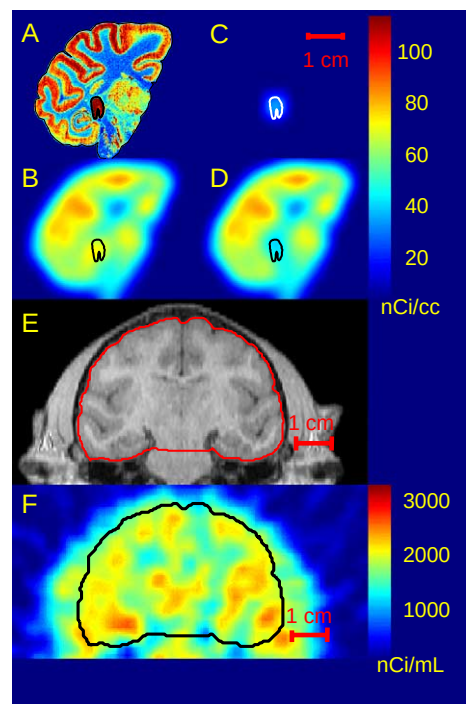

Fig. 3. Sample sections from a three-dimensional autoradiographic database used to estimate PET partial volume effects and sensitivity for detecting changes in rCPS. (A) [^{14}C]Leucine autoradiogram at the level of the lateral geniculate nucleus (LGN). Image is from a 20-μm coronal section of one hemisphere of a monkey brain. (B) Same section after smoothing autoradiographic volume in three dimensions to match the resolution of the GE Advance PET scanner. Outline shows LGN. (C) The LGN volume isolated from the autoradiographic volume and smoothed to the resolution of the PET scanner. Activity outside the outline represents spill out to surrounding tissues in the PET scan. Activity inside the outline originated from the LGN. (D) The remainder volume (i.e., the autoradiographic volume from which the LGN has been removed) smoothed to the resolution of the PET scanner. Because the LGN has been removed from the volume, activity inside the outline represents spill in from surrounding tissues. (E) MR image of another monkey at approximately the same level. (F) Image acquired on the GE Advance PET scanner 45–60 min after injection of 8.3 mCi of L-[1-^{11}C]leucine, coregistered to MR image shown in Panel (E). Data from Panels (A) to (D) can be used to quantitatively estimate partial volume effects in the PET scan, including the recovery coefficient, amount of spill in, amount of spill out and sensitivity of the PET scan for detecting changes in rCPS in the region of interest (see text).

small animal PET [42]. Autoradiographic data may also be useful in predicting whether specific changes will be detectable with PET, as described below.

We have been studying rates of rCPS with the quantitative autoradiographic L-[1-^{14}C]leucine method [3]. Effects of thiopental anesthesia are small [31], suggesting that it may be possible to study rCPS under anesthesia without significant confounding effects. In order to examine the accuracy and sensitivity of the method for use with L-[1-^{11}C]leucine and PET, we have built a three-dimensional volume from L-[1-^{14}C]leucine autoradiograms of one hemisphere of a monkey brain. Twenty-micrometer coronal sections were calibrated for radioactivity and manually aligned from a set of landmarks placed by the operator, and any missing section was inserted by interpolation. The volume was smoothed in three dimensions with a gaussian kernel whose size was determined by the resolution of one of the PET scanners available at our institution, the GE Advance (6.5 mm FWHM in plane; 4.5 mm FWHM axial) (Fig. 3). One can see that the levels of detail in the simulated and actual PET images are fairly comparable. Matching the autoradiographic resolution to the PET allows quantitative comparisons as well: the estimated recovery coefficient is simply the ratio of the activity in the volume of interest (VOI) in the simulated PET volume to that in the autoradiographic volume. For example, in the lateral geniculate nucleus (LGN) illustrated in Fig. 3, the recovery coefficient in the simulated PET image is 54%; this is similar to the 49% ratio of mean rCPS in the LGN directly measured with L-[1-^{11}C]leucine PET and quantitative L-[1-^{14}C]leucine autoradiography in separate animals (unpublished data). The recovery coefficient reflects three factors: activity that originated inside and was detected inside the VOI, activity that originated inside but was detected outside the VOI (spill out) and activity that originated outside but was detected inside the VOI (spill in). These factors can be determined from the autoradiographic database by partitioning the image volume into two parts: the isolated VOI and its complement (the remainder volume). When the isolated VOI is smoothed to the resolution of the PET scanner and the VOI outline from the autoradiogram is placed on the image (Fig. 3C), activity outside the outline represents spill out and activity inside the outline originated from the VOI itself. In the example shown, 81% of the activity of the LGN spilled out to the surrounding areas; only 19% remain inside the VOI in the simulated PET data. Spill in from surrounding tissues can be measured as activity inside the outline of the VOI placed on the smoothed remainder image (Fig. 3D). In the example illustrated, 35% of the activity in the PET image in this VOI originated from surrounding tissues. These factors can be used to assess the sensitivity of PET measurements to changes in rCPS in the VOI under the following conditions. If activity in the VOI changes under test conditions, if the fractional spill out from the VOI is unchanged between baseline and test conditions and if activity in neighboring regions does not change, a sensitivity index S ($0<S<1$) can be derived to indicate the degree to which a change in activity in the VOI would be underestimated in the PET measurement due to partial volume effects. In the LGN of an adult monkey (Fig. 3), for example, the estimated sensitivity index for measurements on the GE Advance scanner is 35%; thus, a hypothetical 20% change in activity in the LGN would be detected as a 35%×20% or only a 7% change in the PET image. In general, with increasing VOI size, the sensitivity for detecting regional changes increases. There are exceptions, however, as the sensitivity index takes factors other than volume into account (i.e., the shape and extent of the region as well as activities in neighboring tissues). The approach can be refined by the addition of a PET noise model and inclusion of any activity that is present in the PET but not in the autoradiographic data. This approach may provide a more useful guide than VOI size alone in making preliminary assessments of whether particular changes in a given region are likely to be detectable with PET without requiring an unacceptably large number of animals.

8. Conclusions

Advances in PET technology have opened up the possibility for performing repeated studies in the same animal and improvements in scanner sensitivity have made single animal kinetic studies achievable. Quantitative autoradiographic data may be useful for making preliminary assessments of whether PET studies are likely to have sufficient power for detecting specific regional changes, but the most formidable challenge remains to devise animal restraint methods that do not mask the effects one is attempting to measure.

References

[1] Sakurada O, Kennedy C, Jehle J, Brown JD, Carbin GL, Sokoloff L. Measurement of local cerebral blood flow with iodo[^{14}C]antipyrine. Am J Physiol 1978;234(1):H59–H66.

[2] Sokoloff L, Reivich M, Kennedy C, Des Rosiers MH, Patlak CS, Pettigrew KD, et al. The [^{14}C]deoxyglucose method for the measurement of local cerebral glucose utilization: theory, procedure, and normal values in the conscious and anesthetized albino rat. J Neurochem 1977;28:897–916.

[3] Smith CB, Deibler GE, Eng N, Schmidt K, Sokoloff L. Measurement of local cerebral protein synthesis in vivo: influence of recycling of amino acids derived from protein degradation. Proc Natl Acad Sci U S A 1988;85:9341–5.

[4] Raichle ME, Martin WRW, Herscovitch P, Mintun MA, Markham J. Brain blood flow measured with intravenous $H_2^{15}O$: II. Implementation and validation. J Nucl Med 1983;24:790–8.

[5] Reivich M, Kuhl D, Wolf A, Greenberg J, Phelps M, Ido T, et al. The [^{18}F]fluorodeoxyglucose method for the measurement of local cerebral glucose utilization in man. Circ Res 1979;44:127–37.

[6] Schmidt KC, Cook MP, Qin M, Kang J, Burlin TV, Smith CB. Measurement of regional rates of cerebral protein synthesis with L-[1-^{11}C]leucine and PET with correction for recycling of tissue amino acids: I. Kinetic modeling approach. J Cereb Blood Flow Metab 2005;25:617–28.

[7] Smith CB, Schmidt KC, Qin M, Burlin TV, Cook MP, Kang J, et al. Measurement of regional rates of cerebral protein synthesis with L-[1-^{11}C]leucine and PET with correction for recycling of tissue amino acids: II. Validation in rhesus monkeys. J Cereb Blood Flow Metab 2005;25:629–40.

[8] Buxton RB. Introduction to functional magnetic resonance imaging. Cambridge, UK: Cambridge University Press; 2002. p. 390–416.

[9] Goldman H. Techniques for the measurement of cerebral blood flow. In: Phillis JW, editor. The regulation of cerebral blood flow. Boca Raton: CRC Press; 1993. p. 3–32.

[10] Sokoloff L. Relationships among local functional activity, energy metabolism, and blood flow in the central nervous system. Fed Proc 1981;40:2311–6.

[11] Zhao W, Young TY, Ginsberg MD. Registration and three-dimensional reconstruction of autoradiographic images by the disparity analysis method. IEEE Trans Med Imaging 1993;12(4):782–91.

[12] Smith CB. Localization of activity-associated changes in metabolism of the central nervous system with the deoxyglucose method: prospects for cellular resolution. In: Barker JL, McKelvy JF, editors. Curr Methods Cell Neurobiol, vol. I: Anatonomical techniques. New York: John Wiley & Sons; 1983. p. 269–317.

[13] Landau WM, Freygang WH, Rowland LP, Sokoloff L, Kety SS. The local circulation of the living brain: values in the unanesthetized and anesthetized cat. Trans Am Neurol Ass 1955;80:125–9.

[14] Kety SS. The theory and applications of the exchange of inert gas at the lungs and tissues. Pharmacol Rev 1951;3:1–41.

[15] Reivich M, Jehle J, Sokoloff L, Kety SS. Measurement of regional cerebral blood flow with antipyrine-14C in awake cats. J Appl Physiol 1969;27(2):296–300.

[16] Jay TM, Lucignani G, Crane AM, Jehle J, Sokoloff L. Measurement of local cerebral blood flow with [^{14}C]iodoantipyrine in the mouse. J Cereb Blood Flow Metab 1988;8:121–9.

[17] Levin CS, Hoffman EJ. Calculation of positron range and its effect on the fundamental limit of positron emission tomography system spatial resolution. Phys Med Biol 1999;44:781–99.

[18] Myers R, Hume S. Small animal PET. Eur Neuropsychopharmacol 2002;12:545–55.

[19] Weber S, Bauer A. Small animal PET: aspects of performance assessment. Eur J Med Mol Imaging 2004;31:1545–55.

[20] Seidel J, Vaquero JJ, Green MV. Resolution uniformity and sensitivity of the NIH ATLAS small animal PET scanner: comparison to simulated LSO scanners without depth-of-interaction capability. IEEE Trans Nucl Sci 2003;50(5):1347–50.

[21] Shimoji K, Ravasi L, Schmidt K, Soto-Montenegro ML, Esaki T, Seidel J, et al. Measurement of cerebral glucose metabolic rates in the anesthetized rat by dynamic scanning with the ^{18}F-FDG, the ATLAS small animal PET scanner, and arterial blood sampling. J Nucl Med 2004;45:665–72.

[22] Shimoji K, Ravasi L, Esaki T, Soto-Montenegro ML, Schmidt K, Seidel J, et al. Use of [^{18}F]FDG and ATLAS small animal PET scanner to study the functional activation in the somatosensory cortex by whisker stimulation in unanesthetized rats. J Nucl Med 2003;44(5 Suppl S):784.

[23] Schmidt K, Shimoji K, Ravasi L, Soto-Montenegro M, Esaki T, Jagoda E, et al. Kinetics of 2-[^{18}F]fluoro-2-deoxyglucose in rat brain estimated from dynamic scanning with the ATLAS small animal PET scanner and arterial blood sampling. J Cereb Blood Flow Metab 2003;23(Suppl 1):673.

[24] Schmidt K, Mies G, Sokoloff L. Model of kinetic behavior of deoxyglucose in heterogeneous tissues in brain: a reinterpretation of the significance of parameters fitted to homogeneous tissue models. J Cereb Blood Flow Metab 1991;11:10–24.

[25] Schmidt K, Lucignani G, Moresco RM, Rizzo G, Gilardi MC, Messa C, et al. Errors introduced by tissue heterogeneity in estimation of local cerebral glucose utilization with current kinetic models of the [^{18}F]fluorodeoxyglucose method. J Cereb Blood Flow Metab 1992;12:823–34.

[26] Schmidt KC, Lucignani G, Sokoloff L. Fluorine-18-fluorodeoxyglucose PET to determine regional cerebral glucose utilization: a reexamination. J Nucl Med 1996;37:394–9.

[27] Lucignani G, Schmidt KC, Moresco RM, Striano G, Colombo F, Sokoloff L, et al. Measurement of regional cerebral glucose utilization with fluorine-18-FDG and PET in heterogeneous tissues: theoretical considerations and practical procedure. J Nucl Med 1993;34:360–9.

[28] Dewar D, McCulloch J. Mapping functional events in the CNS with 2-deoxyglucose autoradiography. In: Stewart MG, editor. Quantitative methods in neuroanatomy. England: John Wiley & Sons; 1992. p. 57–84.

[29] Maekawa T, Tommasino C, Shapiro HM, Keifer-Goodman J, Kohlenberger RW. Local cerebral blood flow and glucose utilization during isoflurane anesthesia in the rat. Anesthesiology 1986;65:141–4.

[30] Szabó L, Kovách AGB, Babose M. Local effect of anesthesia on cerebral blood flow in the rat. Acta Physiologica Hungarica 1983; 62(2):113–21.

[31] Smith CB, Eintrei C, Kang J, Sun Y. Effects of thiopental anesthesia on local rates of cerebral protein synthesis in rats. Am J Physiol 1998;274:E852–9.

[32] Nakao Y, Itoh Y, Kuang T-Y, Cook M, Jehle J, Sokoloff L. Effects of anesthesia on functional activation of cerebral blood flow and metabolism. Proc Natl Acad Sci U S A 2001;98(13):7593–8.

[33] Matsumura A, Mizokawa S, Tanaka M, Wada Y, Nozaki S, Nakamura F, et al. Assessment of microPET performance in analyzing the rat brain under different types of anesthesia: comparison between quantitative data obtained with microPET and ex vivo autoradiography. NeuroImage 2003;20:2040–50.

[34] Tsukada H, Sato K, Kakiuchi T, Nishiyama S. Age-related impairment of coupling mechanism between neuronal activation and functional cerebral blood flow response was restored by cholinesterase inhibition: PET study with microdialysis in the awake monkey brain. Brain Res 2000;857:158–64.

[35] Noda A, Takamatsu H, Minoshima S, Tsukada H, Nishimura S. Determination of kinetic rate constants for 2-[^{18}F]fluoro-2-deoxy-D-glucose and partition coefficient of water in conscious macaques and alterations in aging or anesthesia examined on parametric images with an anatomic standardization technique. J Cereb Blood Flow Metab 2003;23:1441–7.

[36] Hassoun W, LeCavorsin M, Ginovart N, Zimmer L, Gualda V, Bonnefoi F, et al. PET study of the [^{11}C]raclopride binding in the striatum of the awake cat: effects of anaesthetics and role of cerebral blood flow. Eur J Nucl Med 2003;30:141–8.

[37] Zimmer L, Fournet G, Joseph B, Guillaumet G, LeBars D. Carbon-11 labelling of 8{{3-[4-(2-[^{11}C]methoxyphenyl)piperazin-1-yl]-2-hydroxypropyl}oxy}thiochroman, a presynaptic 5-HT_{1A} receptor agonist, and its in vivo evaluation in anaesthetised rat and in awake cat. Nucl Med Biol 2003;30:541–6.

[38] Momosaki S, Hatano K, Kawasumi Y, Kato T, Hosoi R, Kobayashi K, et al. Rat-PET study without anesthesia: anesthetics modify the dopamine D1 receptor binding in rat brain. Synapse 2004;54: 207–13.

[39] Vaska P, Woody CL, Schlyer DJ, Shokouhi S, Stoll SP, Pratte J-F, et al. RatCAP: miniaturized head-mounted PET for conscious rodent brain imaging. IEEE Trans Nucl Sci 2004;51(5):2718–22.

[40] Woody C, Kriplani A, O'Conner P, Pratte J-F, Radeka V, Rescia S, et al. RatCAP: a small, head-mounted PET tomograph for imaging the brain of an awake rat. Nucl Instrum Methods in Phys Res A 2004;527:166–70.

[41] Hoffman EJ, Huang S-C, Phelps ME. Quantitation in positron emission computed tomography: 1. Effect of object size. J Comput Assist Tomogr 1979;3(3):299–308.

[42] Valla J, Chen K, Berndt JD, Gonzalez-Lima F, Cherry SR, Games D, et al. Effects of image resolution on autoradiographic measurements of posterior cingulate activity in PDAPP mice: implications for functional brain imaging studies of transgenic mouse models of Alzheimer's disease. NeuroImage 2002;16:1–6.